LETTER • OPEN ACCESS

Beyond the recharge/discharge paradigm: Pacific meridional mode acts as a critical driver for multi-year La Niña events

To cite this article: Liang Shi *et al* 2026 *Environ. Res. Lett.* **21** 034016

View the article online for updates and enhancements.

ENVIRONMENTAL RESEARCH
LETTERS

Beyond the recharge/discharge paradigm: Pacific meridional mode acts as a critical driver for multi-year La Niña events

Liang Shi[1,2] , Shujuan Hu[3] , Yu-heng Tseng[4] , Jianping Li[5] and Ruiqiang Ding[6,7,*]

[1] Qinghai Provincial Key Laboratory of Plateau Climate Change and Corresponding Ecological and Environmental Effects, Qinghai Institute of Technology, Xining 810016, People's Republic of China
[2] Department of Atmospheric Sciences, School of Ecology and Environmental Science, Qinghai Institute of Technology, Xining 810016, People's Republic of China
[3] Key Laboratory for Semi-Arid Climate Change of the Ministry of Education, College of Atmospheric Sciences, Lanzhou University, Lanzhou 730000, People's Republic of China
[4] Institute of Oceanography, National Taiwan University, Taipei, Taiwan Ocean Center, National Taiwan University, Taipei, Taiwan
[5] Frontiers Science Center for Deep Ocean Multispheres and Earth System (FDOMES)/Key Laboratory of Physical Oceanography/ Institute for Advanced Ocean Studies, Ocean University of China, Qingdao, People's Republic of China
[6] State Key Laboratory of Earth Surface Processes and Resource Ecology, Beijing Normal University, Beijing 100875, People's Republic of China
[7] Key Laboratory of Environmental Change and Natural Disasters of Chinese Ministry of Education/Faculty of Geographical Science, Beijing Normal University, Beijing 100875, People's Republic of China
* Author to whom any correspondence should be addressed.

E-mail: drq@bnu.edu.cn

Abstract

The persistence of multi-year La Niña events (MLa Niñas) drives catastrophic climate anomalies worldwide, yet their initiation and maintenance mechanisms remain poorly understood. The conventional recharge/discharge theory effectively explains MLa Niñas preceded by strong El Niño events (SE-MLa Niñas), but fails to account for MLa Niñas occurring without preceding strong El Niño influences (NSE-MLa Niñas). Here we show, through integrated observational analyses and climate model simulations, that the Pacific meridional mode (PMM) acts as a key driver for the initiation and maintenance of NSE-MLa Niñas. Unlike SE-MLa Niñas, which rely on El Niño-induced oceanic memory, NSE-MLa Niñas are sustained by the PMM-related subtropical air–sea coupling processes, notably through an intensified wind–evaporation–sea surface temperature feedback mechanism as quantitatively diagnosed in this study. Future projections indicate that under global warming scenarios, the frequency of NSE-MLa Niñas may increase more relative to SE-MLa Niñas, possibly due to the enhanced PMM variability. These findings deepen our understanding of ENSO dynamics by uncovering subtropical processes as critical drivers of persistent La Niña conditions, with profound implications for advancing ENSO prediction systems.

1. Introduction

La Niña events (La Niñas), unlike El Niño events (El Niños), are more prone to extend over two or more years, evolving into multi-year La Niña events (MLa Niñas) (Hu *et al* 2013, Timmermann *et al* 2018, Wang *et al* 2023). These extended La Niñas significantly increase the cumulative risk of extreme weather events globally. Manifestations range from severe flooding in Southeast Asia (Raj Deepak *et al* 2019) and northern Australia (Holgate *et al* 2022, Huang

et al 2024) to prolonged droughts and wildfires in the southern United States and parts of South America (Cole 2002, Okumura *et al* 2017). Such events further drive extreme summer heatwaves in East Asia (Iwakiri and Watanabe 2021, Yeo and Kim 2021) and induce marked zonal shifts in Antarctic sea ice concentrations during austral winter (Zhu and Yu 2022). Particularly, the recent 2020–2023 'triple-dip' La Niña exemplifies these impacts, having contributed to persistent flooding in eastern Australia while intensifying droughts in the United States and East Africa

(Jones 2022). Consequently, understanding the mechanisms behind MLa Niñas has therefore become a critical focus in recent ENSO research.

MLa Niñas are often linked to preceding strong El Niños, which are hereafter referred to as SE-MLa Niñas. SE-MLa Niñas have been attributed to a slow recharge process of ocean heat content or warm water volume (WWV) in the tropical Pacific (Wyrtki 1985, Jin 1997, Meinen and McPhaden 2000), as seen in 1998–2000 and 2016–2018 MLa Niñas that followed the 1997 and 2015 super El Niño event, respectively (McPhaden 1999, Wu *et al* 2018, Iwakiri and Watanabe 2021). However, some MLa Niñas often occur with no preceding strong El Niño events (Jones 2022, Kim *et al* 2023, Shi *et al* 2023), which are hereafter referred to as NSE-MLa Niñas. The development and maintenance of these NSE-MLa Niñas cannot be fully accounted by the conventional recharge/discharge mechanism. For instance, Kim *et al* (2023) noted that the recharge/discharge theory (Jin 1997) overemphasized the role of preceding strong El Niños, as approximately 64% of MLa Niñas since 1900 have been NSE-MLa Niñas. Furthermore, recent studies have begun to highlight the role of extratropical processes in driving MLa Niñas. In particular, the Pacific meridional mode (PMM), which is a leading mode of coupled ocean–atmosphere variability in the subtropical Pacific characterized by meridional SST and wind anomalies that can propagate equatorward via wind–evaporation–SST (WES) feedback, has been identified as a key precursor for La Niña development (Amaya 2019, Chiang and Vimont 2004, Zhang *et al* 2014). Kim *et al* (2023) and Shi *et al* (2023) further emphasized the dominant role of PMM-related subtropical anomalies in initiating and sustaining NSE-MLa Niñas, challenging the traditional equatorial-centric view. While existing studies have established the importance of PMM variability in La Niña development, a systematic understanding of its role in NSE-MLa Niñas remains incomplete, especially when compared to the well-established recharge/discharge theory for SE-MLa Niñas (McPhaden 1999, Meinen and Mchaden 2000, Latif *et al* 2015, Iwakiri and Watanabe 2021). Building on earlier findings, this study aims to quantify the distinct roles of North PMM (NPMM) and South PMM (SPMM) throughout the life cycle of NSE-MLa Niñas, delineate the two-way feedback loop between subtropical PMM anomalies and equatorial ENSO dynamics, and project their future changes under high-emission scenarios.

In this study, we analyze observations in combination with climate model data from the Coupled Model Intercomparison Project Phase 6 (CMIP6) to demonstrate that the PMM variability serves as a crucial driver for initiating and sustaining NSE-MLa Niñas. Additionally, our future projections suggest that NSE-MLa Niñas will occur more frequently than SE-MLa Niñas in a warming climate, likely driven by the enhanced PMM variability. By quantifying the strength of the WES feedback, we provide direct evidence for the PMM-driven mechanisms in initiating NSE-MLa Niñas. Our findings underscore the growing significance of PMM variability in diving the initiation and maintenance of MLa Niñas.

2. Data

2.1. Observed data
This study utilizes monthly SST data from three different sources: (1) the Hadley Center Sea Ice and SST dataset version 3 (HadISST) (Rayner *et al* 2006); (2) the Extended Reconstructed SST version 4 from the National Oceanic and Atmospheric Administration (Smith *et al* 2008), and (3) the Kaplan Extended SST version 2 (Kaplan SST) (Kaplan *et al* 1998). Monthly atmospheric fields, including surface winds, u10m winds, latent heat flux (LHF), and shortwave radiation were obtained from the NCEP/NCAR reanalysis 1 (Kalnay *et al* 1996). The oceanic subsurface temperature data at a resolution of $1° \times 1°$ for the period 1980–2024 came from the Institute of Atmospheric Physics (IAP), Chinese Academy of Sciences spanning 1948–2024 was also used (Cheng *et al* 2017), and the NCEP Global Ocean Data Assimilation System (GODAS; Behringer and Xue 2004). All anomalies are computed relative to the climatological annual cycle from 1991 to 2020.

2.2. CMIP6 simulations
To investigate the accuracy and robustness of the role of extratropical Pacific processes in initiating and maintaining NSE-MLa Niñas as indicated by reanalysis data, we here analyzed the historical (1900–1999) simulation outputs from the coupled general circulation models participating in CMIP6 (table S2; Eyring *et al* 2016). Our hypothesis posits that the influence of SE-MLa Niñas and NSE-MLa Niñas arises from a complex interplay of tropical–subtropical interaction processes. Accurate simulation of the SPMM roles in developing these events requires models that effectively capture the NPMM- and SPMM-ENSO connections and the distinct La Niña phenomena. Additionally, we employed simulations under SSP126, 245, and 585 scenarios (2000–2099) to investigate future changes in the frequency of the two types of MLa Niñas and their association with SPMM variability.

3. Methodology

3.1. Definition of MLa Niña
For the observational analysis, an MLa Niña is identified using monthly SST anomalies averaged over the 5° S to 5° N and 120° to 170° W (referred to as the 'Niño3.4 index') for the period 1948–2024 (Wang *et al*

2023). An MLa Niña is characterized by a Niño 3.4 index below −0.5 S.D. in any winter months from October to February from year (0) to year (1), and thereafter remain below zero for at least five consecutive months (Ding *et al* 2022). Based on these criteria, ten MLa Niñas occurred during 1948–2024 (figure 1(a) and table S1). The definitions of MLa Niñas are consistent across both CMIP6 models and observations. Furthermore, a strong (weak) El Niño event is defined as a winter (October (0)–February (1)) Niño34 index greater than or less than 1 S.D. It is important to note that as shown in figure S1, the winter Niño3.4 index from 1900 to 2024 is calculated using three different SST datasets. Considerable discrepancies exist among the datasets prior to 1948, whereas post-1948 ENSO events are largely consistent. Accordingly, all reanalysis-based results in this study are derived from the 1948 to 2024 period.

3.2. NPMM, SPMM, and other related indices
The NPMM index is calculated by the normalized SST anomalies over the region of subtropical northeastern Pacific (15°−25° N and 175° E−90° W) (Amaya 2019, Zheng *et al* 2024). We calculate the SPMM index as the area-averaged SST anomalies over the subtropical South Pacific (15°−25° S, 110°−80° W), following Zhang *et al* (2014). To test robustness, we conducted sensitivity analyses using alternative domains, including a broader range (10°–35° S, You and Furtado 2017). The key patterns and conclusions concerning the SPMM's role in La Niña initiation and persistence remain consistent, confirming that our findings are not sensitive to the precise latitudinal definition and that the identified subtropical influence is physically robust. The WWV index, defined as the volume of water above the 20 °C isotherm between 5° N–5° S and 120° E–80° W (Meinen and McPhaden 2000). Our analysis primarily relied on data from the IAP, Chinese Academy of Sciences (Cheng *et al* 2017), due to its temporal coverage matching our study period. We also derived monthly WWV values using temperature data from the NCEP GODAS; however, since its record begins in 1980, the resulting index served only for reference and validation.

3.3. Statistical significance test
We employed bootstrap method (Austin and Tu 2004) to determine whether the SE-MLa Niñas or NSE-MLa Niñas differs significantly in observational data and CMIP6 simulations. To do this, we randomly resampled the winter of year (−1) Niño34 and WWV indices from SE-MLa Niñas and NSE-MLa Niñas, generating 10 000 realizations for both types of MLa Niñas. In this process, any model could be selected multiple times. This method can also be used to test the significance of the difference between the occurrence frequencies of SE-MLa Niñas and NSE-MLa

Niñas. Additionally, the statistical significance of correlations and composites was evaluated using a two-tailed Student's *t*-test with $n-2°$ of freedom, where n is the number of years.

3.4. Ocean mixed-layer heat budget analysis
We also applied the mixed-layer heat budget analysis as follows:

$$
\begin{aligned}
\frac{\partial T'}{\partial t} = & -\left(\bar{u}\frac{\partial T'}{\partial x} + u'\frac{\partial \bar{T}}{\partial x} + u'\frac{\partial T'}{\partial x} \right) \\
& -\left(\bar{v}\frac{\partial T'}{\partial y} + v'\frac{\partial \bar{T}}{\partial y} + v'\frac{\partial T'}{\partial v} \right) \\
& -\left(\bar{w}\frac{\partial T'}{\partial z} + w'\frac{\partial \bar{T}}{\partial z} + w'\frac{\partial T'}{\partial z} \right) \\
& + \frac{Q}{\rho C_P H} + R_0
\end{aligned}
$$

where T, u, v, and w represent the temperature, zonal current, meridional current, and vertical current, respectively, within a constant mixed layer depth H. The value H is set to 30 m, which corresponds to the climatological mixed layer depth. Q denotes the total surface heat flux; ρ is the seawater density, and C_p is the ocean's heat capacity. R_0 refers to the residual term. Variables with (') represent anomalies, while those with a bar (¯) denote climatology values. The mixed-layer temperature tendency (°C month^{-1}) is primarily driven by three key processes: zonal heat advection (zonal advective feedback; $-u'\partial\bar{T}/\partial x$), vertical heat advection (thermocline feedback; $-\bar{w}\partial T'/\partial z$), and vertical heat advection (upwelling feedback; $-w'\partial\bar{T}/\partial z$). These processes are linked to anomalous zonal currents, vertical shifts in the thermocline, and upwelling, respectively.

3.5. Quantification of WES feedback strength
The strength of WES feedback is estimated following the coupled feedback framework of Xie (1999) and Vimont *et al* (2003). Over the NPMM and SPMM region, we compute monthly anomalies of surface wind speed at 10 m (U10), LHF, and SST. The WES feedback intensity (β_{WES}) is defined as:

$$
\beta_{WES} = -\left(\frac{\partial LHF}{\partial U10} \right) \cdot \left(\frac{\partial SST}{\partial LHF} \right)
$$

where the partial derivatives are derived from linear regression over the onset phase (MAM–JJA) of each MLa Niñas.

4. Results

4.1. Comparisons of SE-MLa Niñas and NSE-MLa Niñas
Since 1948, ten MLa Niñas have been identified, comprising those preceded by strong El Niños (SE-MLa Niñas) and those without preceding strong El Niños

Figure 1. Evolutions of Niño3.4 and WWV indices for SE-MLa and NSE-MLa La Niña events in observations. (a) The October (−1)–February (0) (OND–1JF0) averaged Niño3.4 index (°C) during 1948–2024. Red and blue boxes indicate SE-MLa Niñas and NSE-MLa Niñas, respectively. (b), (c) Time evolutions of the Niño3.4 index (°C) and the WWV index (10^{14} m^3) from year (−1) to year (2) for SE-MLa Niñas and NSE-MLa Niñas. The thick blue and orange lines represent the average evolution of each event type, respectively. (d) Phase space evolutions of the monthly averaged Niño3.4 (x-axis; °C) and WWV (y-axis; m^3) indices during the SE-MLa Niñas and NSE-MLa Niñas. (e), (f) Histograms of 10 000 bootstrap realizations of the OND–JF0 Niño3.4 and May–September (−1) (MJJAS−1) WWV indices for the SE-MLa Niñas and NSE-MLa Niñas. Vertical orange and blue lines indicate the mean values of the 10 000 realizations for each event type. Gray shaded areas represent the 95% confidence intervals, defined as twice the standard deviation of the 10 000 realizations under a normal distribution.

(NSE-MLa Niñas), with a cumulative duration spanning 23 La Niña years (figure 1(a), table S1). The classification results show that over the past 76 years, the occurrence frequency of SE-MLa Niñas and NSE-MLa Niñas is comparable, with each type occurring 5 times. This finding aligns with previous research conclusions (Wang *et al* 2023), challenging the prevailing view that the development of MLa Niñas is predominantly dependent on preceding strong El Niño occurrences. Similarly, although the frequency of NSE-MLa Niñas is lower than that of all La Niña events (figure 1(a)), their occurrence exhibits significant variability. Specifically, in the 53 year period prior to 2000, three such events were recorded, whereas two

events have occurred in the 24 years since 2000. The comparison of these periods reveals an approximately 46% increase in the annual incidence rate of NSE-MLa Niñas after the year 2000, indicating a marked upward trend in their frequency. Notably, one of the two post-2000 events is the only recorded instance of a La Niña preceded by a weak El Niño, further exemplifying that such atypical NSE-MLa Niñas have become more frequent during this recent period of heightened activity.

The composite evolutions of the Niño3.4 and WWV indices for SE-MLa Niñas and NSE-MLa Niñas, covering the year before El Niño (−1), and the La Niña onset (0), the year following onset (1), and
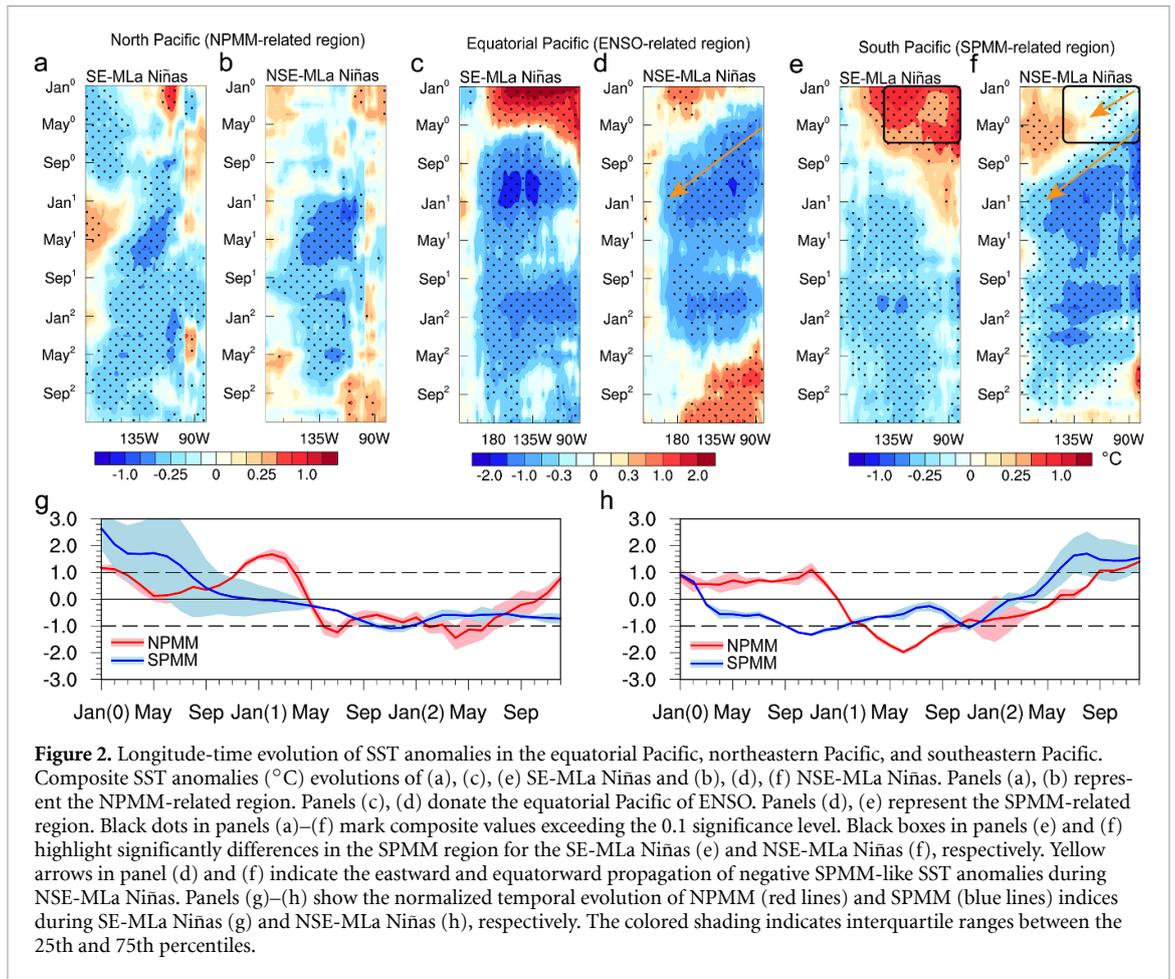
Figure 2. Longitude-time evolution of SST anomalies in the equatorial Pacific, northeastern Pacific, and southeastern Pacific. Composite SST anomalies (°C) evolutions of (a), (c), (e) SE-MLa Niñas and (b), (d), (f) NSE-MLa Niñas. Panels (a), (b) represent the NPMM-related region. Panels (c), (d) donate the equatorial Pacific of ENSO. Panels (d), (e) represent the SPMM-related region. Black dots in panels (a)–(f) mark composite values exceeding the 0.1 significance level. Black boxes in panels (e) and (f) highlight significantly differences in the SPMM region for the SE-MLa Niñas (e) and NSE-MLa Niñas (f), respectively. Yellow arrows in panel (d) and (f) indicate the eastward and equatorward propagation of negative SPMM-like SST anomalies during NSE-MLa Niñas. Panels (g)–(h) show the normalized temporal evolution of NPMM (red lines) and SPMM (blue lines) indices during SE-MLa Niñas (g) and NSE-MLa Niñas (h), respectively. The colored shading indicates interquartile ranges between the 25th and 75th percentiles.

the year of decay (2), are shown in figures 1(b) and (c). SE-MLa Niñas are characterized by an averaged Niño3.4 index of 2.2 °C (figure 1(b)) from October (−1) to February (0) (OND–1JF0) and a mean WWV index of 1.8×10^{14} m^3 (figure 1(c)) from May (−1) to September (−1) (MJJAS–1). In contrast, NSE-MLa Niñas exhibit significantly weaker indices, with an average Niño3.4 index of 0.45 °C (figure 1(b)) during OND–1JF0 and a WWV index of 0.3×10^{14} m^3 during MJJAS–1 (figure 1(c)), representing approximately one-sixth the intensity of these indices observed in the preceding El Niños of SE-MLa Niñas. These differences in both the Niño3.4 and WWV indices between SE-MLa Niñas and NSE-MLa Niñas are significant at the 99% confidence level (figures 1(e) and (f)). Additionally, there exists a significant lead-lag relationship between the WWV and Niño3.4 indices during SE-MLa Niñas, with the WWV index leading by two to three seasons (figure 1(d)). This suggests that the initiation and maintenance of SE-MLa Niñas are closely associated with a pronounced and strong discharge process in the equatorial Pacific (Wu *et al* 2018, Iwakiri and Watanabe 2021). However, no such lead-lag relationship is observed between the WWV and Niño3.4 indices throughout the entire cycle of NSE-MLa Niñas, particularly during the

period during year (−1) to year (0). Moreover, the intensity of the WWV index does not align with the intensity of subsequent La Niñas in year (0) and (1), respectively (figure 1(d)). This suggests a much weaker discharge process in the equatorial Pacific during NSE-MLa Niñas.

4.2. The PMM mechanism for the formation of the NSE-MLa Niñas

Previous studies have shown that PMM variability (including both the NPMM and SPMM, through tropical–subtropical interactions, can effectively initiate ENSO variability (Jia *et al* 2021, Park *et al* 2021, Kim *et al* 2023, Shi *et al* 2023). The SST anomalies associated with these PMMs propagate equatorward through the WES feedback (Xie 1999, Vimont *et al* 2003), where these anomalous can facilitate LHFs and reinforce meridional SST gradients. In the case of NSE-MLa Niñas, the WES-mediated propagation is visually depicted in figure 2(f) (yellow arrows). However, research on these PMM precursors has primarily focused on their effects on the onset of general ENSO events (Amaya 2019, Zhang *et al* 2014, You and Furtado 2017, Ding *et al* 2022), while less attention has been paid to the distinct role of the PMM in the sustained evolution and multi-year persistence of

NSE-MLa Niñas. Although recent studies (e.g. Kim *et al* 2023, Shi *et al* 2023) have clearly demonstrated the central role of the PMM in triggering these events, the mechanisms by which the PMM contributes to their unique prolonged lifecycle, in contrast to canonical ENSO events, require further examination. This study specifically focuses on these unresolved aspects.
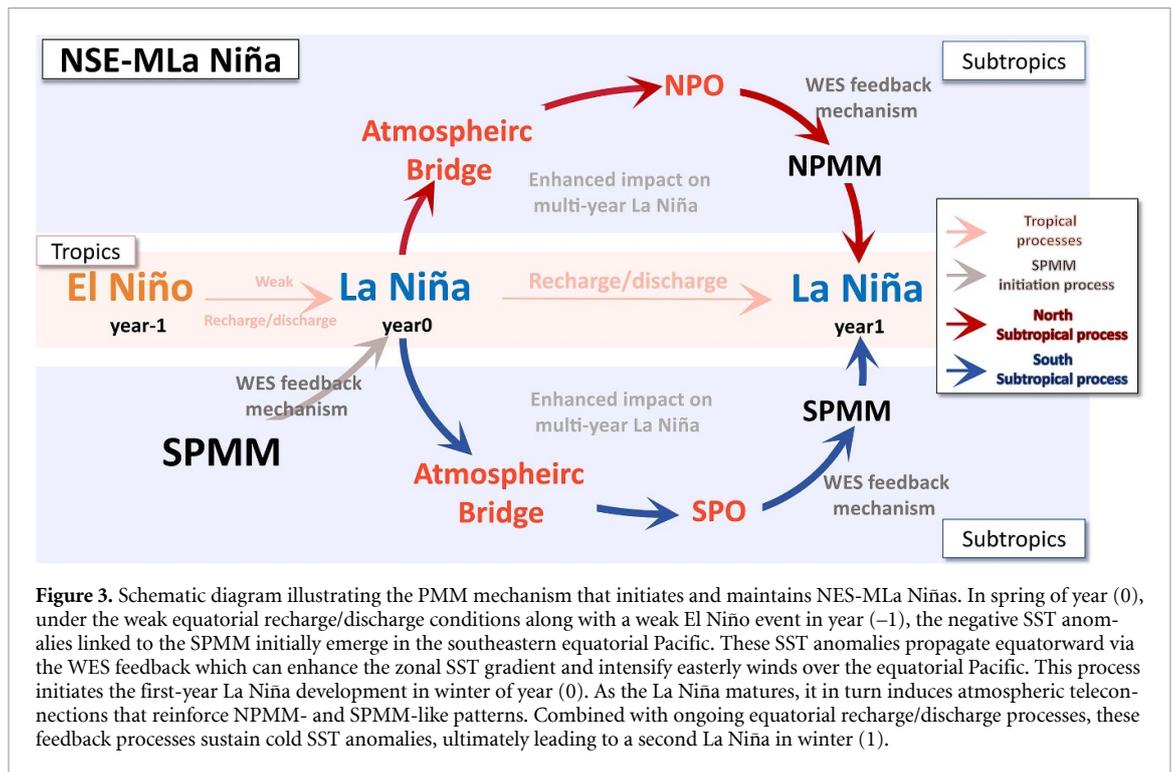
Figures 2(a)–(f) presents the composite evolutions of SST anomalies in the subtropical North Pacific (NPMM-related region; 15° N–25° N, 180°–80° W; figures 2(a) and (b)), equatorial Pacific (5° N–5° S, 140° E–80° W; figures 2(c) and (d)), and subtropical South Pacific (SPMM-related region; 15° S–25° S, 110°–80° W; figures 2(e)–(f)) for SE-MLa Niñas and NSE-MLa Niñas. For SE-MLa Niñas, accompanied by a strong discharge process in the equatorial Pacific following the decay of strong El Niños in year (−1) (figure 2(c)), negative SST and easterly wind anomalies rapidly emerge in the central equatorial Pacific during spring of year (0) (figure S2). Meanwhile, subsurface cold-water anomalies accumulate in the central equatorial Pacific, subsequently propagating eastward and upward along the thermocline (figure S3). These anomalies together reinforce the thermocline and zonal advection feedbacks (Bjerknes 1969), with thermocline feedback playing a dominant role (figure S4(a)), thereby driving the formation of the first-year La Niña in winter of year (0) (figure 2(c) and figure S2). Subsequently, the prolonged oceanic adjustment, caused by the extended recovery period of the strong discharge process during year (1), would maintain negative SST anomalies in the equatorial Pacific, ultimately leading to the recurrence of La Niña conditions in the subsequent periods (figures 2(c) and S3).

In contrast, due to the weak discharge processes in the equatorial Pacific (figures 1(d), 4 and S5), the initiation of NSE-MLa Niñas appears to be more strongly influenced by subtropical processes (figures 2(f) and (h)). Specifically, following the decay of weak El Niños during winter of year (−1) (figure 2(d)), negative SST anomalies do not first emerge in the eastern equatorial Pacific, but rather begin to appear in the southeastern Pacific regions associated with the SPMM during the early spring of year (0), gradually intensifying over time (figures 2(f), S6 and S7). Then, these SPMM-related negative SST anomalies propagate from the southeastern Pacific into the equatorial eastern Pacific via the WES feedback (yellow arrows in figure 2(f); see also figures S6 and S7). To further quantify the evolution of the SPMM-related anomalies during NSE-MLa Niñas, we examine the difference between their early and mature developmental phases (figures 2 and S6). The difference fields in SST and surface winds are statistically significant ($p < 0.05$) over the southeastern subtropical Pacific and the equatorial eastern Pacific (figure S8). This statistically robust

progression confirms that the SPMM signal not only emerges in the subtropics but undergoes a significant amplification and equatorward extension as the event matures, reinforcing its role in initiating and sustaining tropical cooling.

The coupling strength of this feedback is quantified in figure S9, which shows the area-averaged β_{WES} computed over the SPMM domain region during MAM (0)–JJA (0). The magnitude of β_{WES} is much larger in NSE-MLa Niñas than in SE-MLa Niñas (differences significant at $p < 0.05$ in figure S10(a) and differences significant at only $p < 0.2$ in figure S10(b)), especially during year (0), confirming the dominance of WES dynamics in initiating these NSE-MLa Niñas. Furthermore, the distinct air–sea coupling processes associated with NPMM and SPMM are illustrated in figure S11, where regression analyses reveal that SPMM variability is more strongly linked to LHF anomalies (consistent with WES feedback), whereas NPMM variability shows a closer relationship with shortwave radiation changes. These anomalies subsequently intensify the zonal SST gradient in the tropical Pacific, thereby strengthening the anomalous easterly winds. The enhanced easterlies in turn amplify both zonal advection and thermocline feedbacks, with the zonal advection feedback (particularly that associated with the SPMM playing a dominant role; figures S4(b) and 11) (Bjerknes 1969). These processes ultimately culminate in the occurrence of the occurrence of the first La Niña during the winter of year (0).

As previous studies have shown, the development of a La Niña event can usually trigger extratropical variability similar to the North Pacific Oscillation (NPO) (Rogers 1981) or South Pacific Oscillation (SPO) (Salinger *et al* 2001) through remote teleconnections (Anderson 2003, Vimont *et al* 2003). Therefore, after the first-year La Niña event develops, it excites these NPO and SPO atmospheric variabilities, subsequently inducing negative SST anomalies analogous to the NPMM and SPMM in the subtropical Northeastern and Southeastern Pacific, thereby contributing to sustain persistent La Niña conditions (Kim and Yu 2020, Geng *et al* 2023, Shi *et al* 2023). Critically, recent work highlights that the efficiency of this reverse feedback depends on the intensity and spatial pattern of the La Niñas (Fan *et al* 2022). In our NSE-MLa Niñas, the La Niña that matures in winter (0) possesses a spatial structure, characterized by persistent cooling extending into the central-to-eastern equatorial Pacific, which effectively projects its signal into the subtropics via an atmospheric bridge (Alexander *et al* 2002). This induces a local atmospheric circulation response conducive to negative sea-level pressure and wind anomalies over the subtropical Pacific, reinforcing negative SST anomalies there through the WES feedback and thus closing a two-way feedback loop. Notably, as

Figure 3. Schematic diagram illustrating the PMM mechanism that initiates and maintains NES-MLa Niñas. In spring of year (0), under the weak equatorial recharge/discharge conditions along with a weak El Niño event in year (−1), the negative SST anomalies linked to the SPMM initially emerge in the southeastern equatorial Pacific. These SST anomalies propagate equatorward via the WES feedback which can enhance the zonal SST gradient and intensify easterly winds over the equatorial Pacific. This process initiates the first-year La Niña development in winter of year (0). As the La Niña matures, it in turn induces atmospheric teleconnections that reinforce NPMM- and SPMM-like patterns. Combined with ongoing equatorial recharge/discharge processes, these feedback processes sustain cold SST anomalies, ultimately leading to a second La Niña in winter (1).
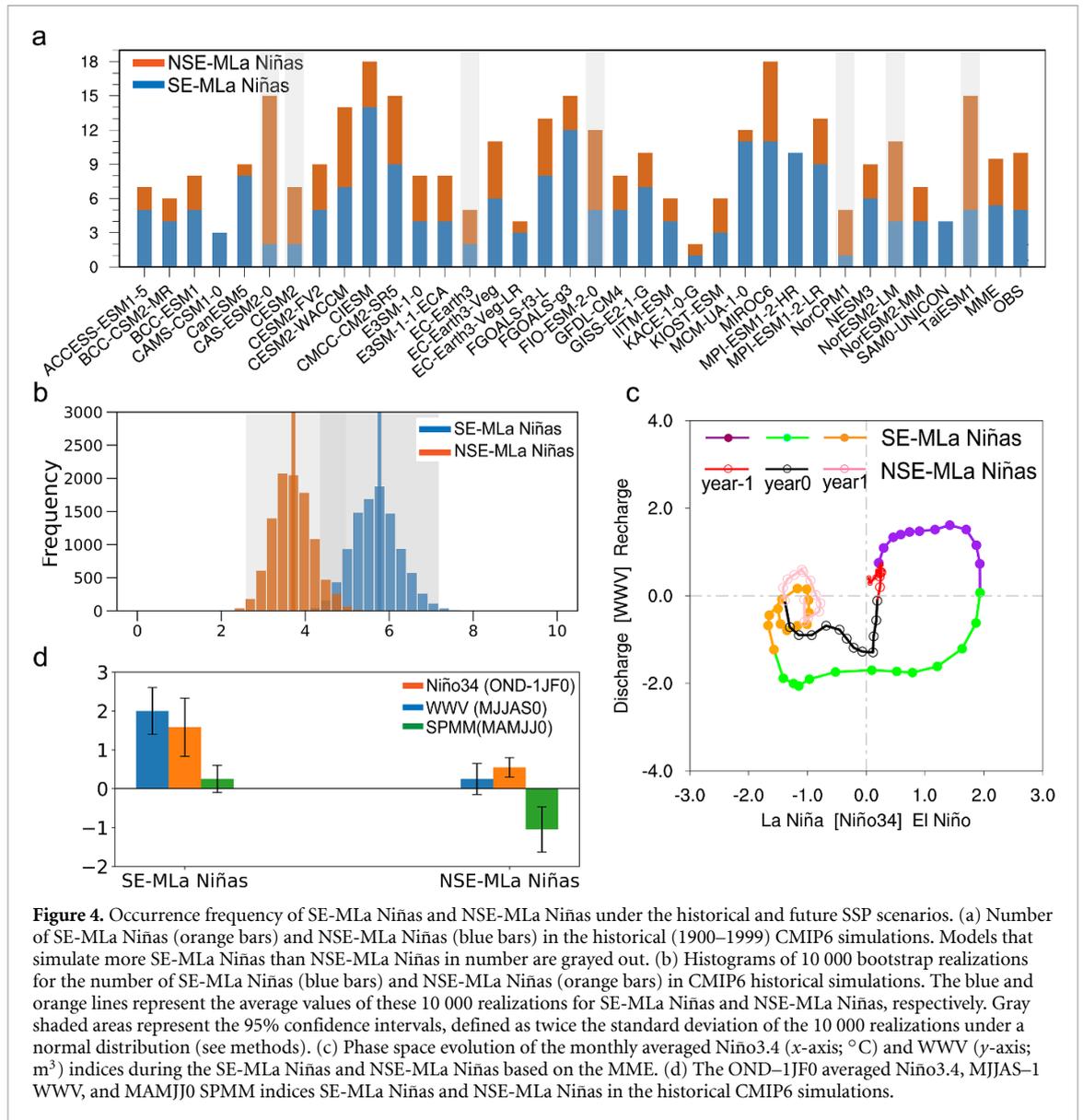
revealed by Fan *et al* (2023), a large PMM index can arise even from strong tropical SST anomalies alone, cautioning against interpreting the index solely as a measure of subtropical variability. In our framework, this means the La Niña-induced subtropical response—even if the resultant subtropical SST anomalies are not extreme—can project effectively onto the canonical PMM pattern, resulting in a persistently negative phase in the index and reinforcing the statistical–dynamical linkage between the tropics and subtropics.

Therefore, the development of the first-year La Niña event excites North and South Pacific atmospheric variability (e.g. NPO and SPO), which subsequently induces PMM-like negative SST anomalies in the subtropical Pacific, contributing to sustained La Niña conditions (Kim and Yu 2020, Geng *et al* 2023, Shi *et al* 2023). This indicates that subtropical processes likely support both the onset and persistence of NSE-MLa Niñas.

The evolution of the NPMM and SPMM indices further differentiates the SE-MLa Niñas and NSE-MLa Niñas. For SE-MLa Niñas (figure 2(g)), both PMM indices align in phase with La Niña development only from year (1) onward, and their overall signal remains weak (or off phase) in year (0), suggesting limited sustained subtropical–tropical coupling this period. In contrast, for NSE-MLa Niñas (figure 2(h)), the SPMM index is already in phase with La Niña from year (0), while the NPMM synchronizes from year (1). Both indices exhibit stronger and more per-

sistent anomalies that co-evolve with the MLa Niña, indicating an active feedback loop in which the initial La Niña reinforces subtropical anomalies that help prolong its duration. This early SPMM phase alignment and its distinct spatial origin—cooling developing in the subtropical southeastern Pacific alongside coherent wind anomalies—suggest active local air–sea coupling. This coupled, subtropical origin differs fundamentally from coastal, ocean-propagated ENSO onset, indicating that the early SPMM acts as an independent subtropical forcing mechanism in NSE-MLa Niñas. A schematic summary of the PMM mechanism presented above is presented in figure 3, illustrating how subtropical PMM variability initiates and sustains NSE-MLa Niñas through coupled ocean–atmosphere processes that link the subtropics and tropics. During winter (−1), the weakened recharge/discharge process in the tropical Pacific enables negative SST anomalies associated with the SPMM to propagate toward the eastern equatorial Pacific through the WES feedback. These anomalies modify the zonal SST gradient and strengthen easterly winds, creating favorable conditions for the development of the first La Niña event during winter of year (0). The maturing La Niña event can trigger atmospheric teleconnections (NPO- and SPO-like variabilities), which reinforce NPMM- and SPMM-like SST patterns. These patterns interact with recharge/discharge dynamics in the equatorial Pacific, sustaining cold SST anomalies into winter of year (1) and ultimately forming an MLa Niña.
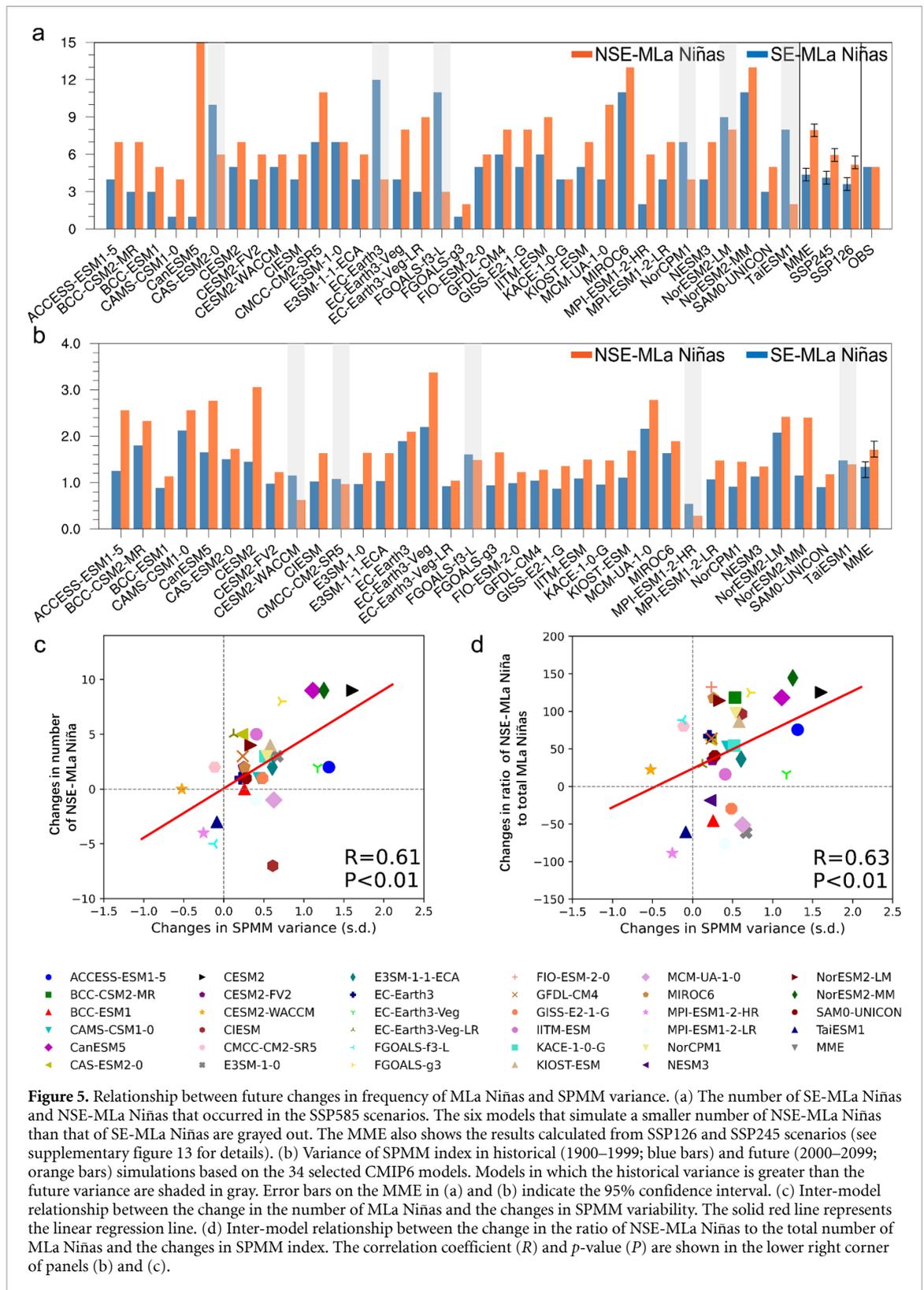
Figure 4. Occurrence frequency of SE-MLa Niñas and NSE-MLa Niñas under the historical and future SSP scenarios. (a) Number of SE-MLa Niñas (orange bars) and NSE-MLa Niñas (blue bars) in the historical (1900–1999) CMIP6 simulations. Models that simulate more SE-MLa Niñas than NSE-MLa Niñas in number are grayed out. (b) Histograms of 10 000 bootstrap realizations for the number of SE-MLa Niñas (blue bars) and NSE-MLa Niñas (orange bars) in CMIP6 historical simulations. The blue and orange lines represent the average values of these 10 000 realizations for SE-MLa Niñas and NSE-MLa Niñas, respectively. Gray shaded areas represent the 95% confidence intervals, defined as twice the standard deviation of the 10 000 realizations under a normal distribution (see methods). (c) Phase space evolution of the monthly averaged Niño3.4 (*x*-axis; °C) and WWV (*y*-axis; m^3) indices during the SE-MLa Niñas and NSE-MLa Niñas based on the MME. (d) The OND–1JF0 averaged Niño3.4, MJJAS–1 WWV, and MAMJJ0 SPMM indices SE-MLa Niñas and NSE-MLa Niñas in the historical CMIP6 simulations.

4.3. Simulated impacts of the PMM on NSE-MLa Niñas

Historical simulations (1900–1999) from 34 selected CMIP6 models provide compelling evidence for the key role of PMM-related processes in initiating and maintaining NSE-MLa Niñas (figure 4). Despite inter-model variability in the frequency of MLa Niñas occurrence, most models successfully reproduce both SE-MLa Niñas and NSE-MLa Niñas (figure 4(a)). The multi-model ensemble (MME) reveals a near-equal partition of MLa Niñas events—52% classified as SE-MLa Niñas and 48% as NSE-MLa Niñas—a result that closely aligns with observational estimates (figure 4(a) and S12). Bootstrap tests further confirm that the difference between these two types is not statistically significant (figure 4(b)).

In CMIP6 models, SE-MLa Niñas are characterized by pronounced anomalies in both Niño3.4 and

WWV indices during their growth and persistence phases (figure 4(d) and figure S13). The phase-space trajectories of WWV versus Niño3.4 indices reveal a distinct lead-lag relationship, indicative of a robust recharge/discharge process (figure 4(c)). Meanwhile, the SST anomalies associated with the SPMM and NPMM are much weaker compared with those in the equatorial Pacific (figures 4(d) and S14).

By contrast, NSE-MLa Niñas exhibit significantly weaker Niño3.4 and WWV indices during year (−1), with no clear phase coherence between the two indices. This suggests a weakened recharge/discharge process in the equatorial Pacific (figures 4(c), (d) and S15). Furthermore, these events feature pronounced subtropical SPMM signal during spring of year (0), with the absolute value of the SPMM index exceeding 1.1 (figures 4(d), S15 and S16). Prominent SPMM-related SST anomalies persist into summer of year

Figure 5. Relationship between future changes in frequency of MLa Niñas and SPMM variance. (a) The number of SE-MLa Niñas and NSE-MLa Niñas that occurred in the SSP585 scenarios. The six models that simulate a smaller number of NSE-MLa Niñas than that of SE-MLa Niñas are grayed out. The MME also shows the results calculated from SSP126 and SSP245 scenarios (see supplementary figure 13 for details). (b) Variance of SPMM index in historical (1900–1999; blue bars) and future (2000–2099; orange bars) simulations based on the 34 selected CMIP6 models. Models in which the historical variance is greater than the future variance are shaded in gray. Error bars on the MME in (a) and (b) indicate the 95% confidence interval. (c) Inter-model relationship between the change in the number of MLa Niñas and the changes in SPMM variability. The solid red line represents the linear regression line. (d) Inter-model relationship between the change in the ratio of NSE-MLa Niñas to the total number of MLa Niñas and the changes in SPMM index. The correlation coefficient (R) and p-value (P) are shown in the lower right corner of panels (b) and (c).

(1), helping to trigger La Niña conditions in year (0) and sustain them into the subsequent year, ultimately forming an MLa Niña event. These modeling results support the observational analysis, indicating that subtropical PMM variability may play an important role in the initiation and maintenance of NSE-MLa Niñas.

4.4. Projections for future climate changes
Recent studies have documented a marked increase in the frequency of MLa Niñas over recent decades (Timmermann *et al* 2018, Ding *et al* 2022, Geng *et al* 2023, Wang *et al* 2023). Given the distinct formation mechanisms of SE-MLa Niñas and NSE-MLa Niñas, this raises an important question: how the

relative occurrence of these two types responds under future warming scenarios. To address this, we conduct a comprehensive analysis based on simulations from 34 CMIP6 models (Eyring *et al* 2016), comparing the frequency changes of SE-MLa Niñas and NSE-MLa Niñas between the historical period (1900–1999) and future projections (2000–2099). This analysis covered three Shared Socioeconomic Pathways (SSP126, SSP245, and SSP585; figure 5).

More than 70% of the models' project that the frequency of MLa Niñas will show an increasing trend relative to historical simulations across all SSP scenarios (figure 5(a)) illustrates results for SSP585; outcomes for SSP126 and SSP245 are presented in figure S17), consistent with previous findings (Jia *et al* 2021, Ding *et al* 2022, Fan *et al* 2023, Geng *et al* 2023). In particular, under the high-emission SSP585 scenario, 28 out of 34 models (over 80%) project that the number of NSE-MLa Niñas will exceed that of SE-MLa Niñas (figure 5(a)). The MME results indicate that SE-MLa Niñas will moderately increase by 25% (from approximately 4 events to 5 events per 100 years), whereas NSE-MLa Niñas will sharply rise by 60% (from about 5 events to 8 events per 100 years). These results show that the projected increase in the frequency of MLa Niñas is primarily attributed to the accelerated increase in NSE-MLa Niñas. Furthermore, as the warming forcing intensifies, NSE-ML La Niña events constitute an increasingly dominant proportion of all MLa Niñas (figures 5(a), S12 and S17) the bootstrap test also verifies this increased change (figures S18).

Given the important role of the SPMM in initiating NSE-MLa Niñas, we examine whether the projected increase in NSE-MLa Niñas frequency under future climate scenarios is dynamically linked to the intensification of SPMM variability. We analyze changes in the boreal spring SPMM variability during MLa Niñas across the 34 CMIP6 models (figure 5(b)). Notably, under the SSP585 scenario, 29 out of 34 models show significantly enhanced SPMM variability relative to historical baselines, with the MME indicating a 28.6% increase (with a change that is statistically significant at the 95% confidence level). Inter-model correlation analysis reveals that models with greater SPMM intensification consistently produce more NSE-MLa Niñas ($R = 0.61$; figure 5(c)). Additionally, a positive correlation is found between SPMM variability and the ratio of NSE-MLa Niñas within all MLa Niñas ($R = 0.63$; figure 5(d)). These findings indicate that anthropogenic warming can enhance SPMM variability through thermodynamic and dynamic pathways (Zhang *et al* 2014, You and Furtado 2017, Ding *et al* 2022, Shi *et al* 2023), thereby promoting the development of NSE-MLa La Niña events.

5. Conclusion and discussion

We demonstrate that subtropical–tropical interactions linked to the PMM are central to initiating and sustaining NSE-MLa Niñas. Unlike SE-MLa Niñas, which mainly rely on preceding ENSO-induced oceanic memory, NSE-MLa Niñas are usually initiated by enhanced SPMM-related SST anomalies. These anomalies can propagate equatorward via the WES feedback, strengthening equatorial easterly wind anomalies and promoting the initiator of first-year La Niña in year (0) (figure 2). This La Niña then feeds back onto both NPMM-like and SPMM-like SST anomalies via atmospheric teleconnections, which, together with recharge/discharge dynamics of the equatorial Pacific, amplify cold SST anomalies and drive a second-year La Niña in year (1), ultimately giving rise to an MLa Niña event. CMIP6 simulations robustly support this mechanism (figure 3). Furthermore, the enhanced WES feedback intensity (β_{WES}) during NSE-MLa Niñas onset provide direct quantitative support for the dual-role mechanism outlined in figure 3. These diagnostics reinforce that subtropical processes are not merely ancillary but are fundamental to the initiation and multi-year persistence of La Niña events without preceding strong El Niño forcing.

Our results further reveal a pronounced climate-state dependence. Under high-emission scenarios, NSE-MLa Niñas are projected to prevail more frequently than SE-MLa Niñas, particularly under SSP585, in line with intensified SPMM variability (figure 5). This shift highlights the leading role of subtropical variability—rather than equatorial dynamics alone—in shaping MLa Niñas. The enhanced SPMM variability under future warming is likely tied to changes in the mean-state background. Specifically, projections indicate a pronounced warming over the southeastern Pacific in CMIP6 models (Fan *et al* 2022), which strengthens the climatological SST gradient and facilitates the meridional WES feedback essential for SPMM growth (Zhang *et al* 2022). This altered mean state may precondition the subtropical Pacific for stronger, more frequent SPMM-like anomalies, thereby promoting NSE-MLa Niña events (Fan *et al* 2023). The sensitivity of this mechanism to anthropogenic forcing underscores the importance of subtropical–tropical coupling in future climate variability, with implications for both prediction and global impact assessment.

While this study elucidates a dual role of the SPMM in both initiating NSE-MLa Niñas and, together with the NPMM, sustaining their persistence. It is also noteworthy that the linkage between the PMM and ENSO may be modulated by low-frequency climate variability (e.g. the Pacific decadal

oscillation, PDO, Stuecker 2018) and other inter-basin processes. Preliminary analysis suggests that the SPMM-triggering mechanism for NSE-MLa Niñas might be more active during cold phases of the PDO. Furthermore, evidence indicates that inter-basin drivers such as the Indian Ocean Dipole (IOD, Ashok *et al* 2001), north tropical Atlantic (NTA, Ham *et al* 2013) SST anomalies, and cross-equatorial wind stresses (Wu *et al* 2018, Zhang *et al* 2024) can also modulate ENSO evolution—for instance, the exceptional 2020–2023 triple-dip La Niña event has been linked to concurrent variability in the IOD and NTA (Hasan *et al* 2022). Quantitatively elucidating the relative contributions and interactions of these decadal and inter-basin modulators with the PMM–ENSO connection requires longer-term observations and model experiments capable of resolving multi-scale interactions, which represents an important avenue for future research toward a more comprehensive understanding of ENSO duration and diversity.

Data availability statement

Acknowledgments

Author contributions

Liang Shi 🄳 0000-0001-6720-1649
Data curation (lead), Formal analysis (lead), Funding acquisition (lead), Investigation (lead), Methodology (lead), Writing – original draft (lead)

Yu-heng Tseng
Supervision (supporting), Validation (supporting), Visualization (supporting)

Jianping Li 🄳 0000-0003-0625-1575
Supervision (supporting), Validation (supporting)

Ruiqiang Ding 🄳 0000-0003-4139-3843
Conceptualization (lead), Funding acquisition (supporting), Methodology (lead), Resources (lead), Supervision (lead), Writing – review & editing (lead)

References

Alexander M A, Blade I, Newman M, Lanzante J R, Lau N-C and Scott J D 2002 The atmospheric bridge: the influence of ENSO teleconnections on air-sea interaction over the global oceans *J. Clim.* **15** 2205–31

Amaya D J 2019 The Pacific meridional mode and ENSO: a review *Curr. Clim. Change Rep.* **5** 296–307

Anderson B T 2003 Tropical Pacific sea-surface temperatures and preceding sea level pressure anomalies in the subtropical North Pacific *J. Geophys. Res. Atmos.* **108** 4732

Ashok K, Guan Z and Yamagata T 2001 Impact of the Indian Ocean dipole on the relationship between the Indian monsoon rainfall and ENSO *Geophy. Res. Lett.* **28** 4499–502

Austin P C and Tu J V 2004 Bootstrap methods for developing predictive models *Am. Stat.* **58** 131–7

Behringer D and Xue Y 2004 Evaluation of the global ocean data assimilation system at NCEP: the Pacific Ocean *8th Symp. on Integrated Observing And Assimilation Systems for Atmosphere, Oceans, and Land Surface 2004*

Bjerknes J 1969 Atmospheric teleconnections from the equatorial Pacific. *Mon. Wea. Rev.* **97** 163–72

Cheng L, Trenberth K, Fasullo J, Boyer T, Abraham J and Zhu J 2017 Improved estimates of ocean heat content from 1960 to 2015 *Sci. Adv.* **3** e1601545

Chiang J C H and Vimont D J 2004 Analogous Pacific and Atlantic meridional modes of tropical atmosphere-ocean variability *J. Clim.* **17** 4143–58

Cole J E 2002 Multiyear La Niña events and persistent drought in the contiguous United States *Geophys. Res. Lett.* **29** 1647

Ding R *et al* 2022 Multi-year El Niño events tied to the North Pacific oscillation *Nat. Commun.* **13** 3871

Eyring V, Bony S, Meehl G A, Senior C A, Stevens B, Stouffer R J and Taylor K E 2016 Overview of the coupled model intercomparison project phase 6 (CMIP6) experimental design and organization *Geosci. Model Dev.* **9** 1937–58

Fan H, Yang S, Wang C and Lin S 2023 Revisiting the impacts of tropical pacific. SST anomalies on the pacific meridional mode during the decay of strong Eastern Pacific El Niño events *J. Clim.* **36** 4987–5002

Fan H, Yang S, Wang C, Wu Y and Zhang G 2022 Strengthening amplitude and impact of the Pacific meridional mode on ENSO in the warming climate depicted by CMIP6 models *J. Clim.* **35** 5195–213

Geng T, Jia F, Cai W, Wu L, Gan B, Jing Z, Li S and McPhaden M J 2023 Increased occurrences of consecutive La Niña events under global warming *Nature* **619** 774–81

Ham Y G, Kug J S, Park J Y and Jin F F 2013 Sea surface temperature in the north tropical Atlantic as a trigger for El Niño/Southern oscillation events *Nat. Geosci.* **6** 112–6

Hasan N A, Chikamoto Y and McPhaden M J 2022 The influence of tropical basin interactions on the 2020–22 double-dip La Niña *Front. Clim.* **4** 1001174

Holgate C, Evans J P, Taschetto A S, Gupta A S and Santoso A 2022 The impact of interacting climate modes on East Australian precipitation moisture sources *J. Clim.* **35** 3147–59

Hu Z-Z, Kumar A, Xue Y and Jha B 2013 Why were some La Niñas followed by another La Niña? *Clim. Dyn.* **42** 1029–42

Huang A T, Gillett Z E and Taschetto A S 2024 Australian rainfall increases during multi-year La Niña *Geophys. Res. Lett.* **51** e2023GL106939

Iwakiri T and Watanabe M 2021 Mechanisms linking multi-year La Niña with preceding strong El Niño *Sci. Rep.* **11** 17465

Jia F, Cai W, Gan B, Wu L and Di Lorenzo E 2021 Enhanced North Pacific impact on El Niño/Southern oscillation under greenhouse warming *Nat. Clim. Change* **11** 840–7

Jin F F 1997 An equatorial ocean recharge paradigm for ENSO. Part I: conceptual model *J. Atmos. Sci.* **54** 811–29

Jones N 2022 Rare 'triple' La Niña climate event looks likely–what does the future hold? *Nature* **607** 21

Kalnay E *et al* 1996 The NCEP–NCAR 40-year reanalysis project *Bull. Am. Meteor. Soc.* **77** 437–71

Kaplan A, Cane M A, Kushnir Y, Clement A C, Blumenthal M B and Rajagopalan B 1998 Analyses of global sea surface temperature 1856–1991 *J. Geophys. Res.* **103** 18567–89

Kim J W and Yu J Y 2020 Understanding reintensified multiyear El Niño events *Geophys. Res. Lett.* **47** e2020GL087644

Kim J W, Yu J Y and Tian B 2023 Overemphasized role of preceding strong El Niño in generating multi-year La Niña events *Nat. Commun.* **14** 6790

Latif M, Semenov V A and Park W 2015 Super El Niños in response to global warming in a climate model *Clim. Change* **132** 489–500

McPhaden M J 1999 Genesis and evolution of the 1997–98 El Niño *Science* **283** 950–4

Meinen C S and McPhaden M J 2000 Observations of warm water volume changes in the equatorial Pacific and their relationship to El Niño and La Niña *J. Clim.* **13** 3551–9

Okumura Y M, DiNezio P N and Deser C 2017 Evolving impacts of multiyear La Niña events on atmospheric circulation and U.S. drought *Geophys. Res. Lett.* **44** 11614–23

Park J H, An S I, Kug J S, Yang Y M, Li T and Jo H S 2021 Mid-latitude leading double-dip La Niña *Int. J. Climatol.* **41** E1353–70

Raj Deepak S N, Chowdary J S, Dandi A R, Srinivas G, Parekh A, Gnanaseelan C and Yadav R K 2019 Impact of multiyear La Niña events on the South and East Asian summer monsoon rainfall in observations and CMIP5 models *Clim. Dyn.* **52** 6989–7011

Rayner N A, Brohan P, Parker D E, Folland C K, Kennedy J J, Vanicek M, Ansell T J and Tett S F B 2006 Improved analyses of changes and uncertainties in sea surface temperature measured *in situ* since the mid-nineteenth century: the HadSST2 dataset *J. Clim.* **19** 446–69

Rogers J C 1981 The North Pacific oscillation *J. Clim.* **1** 39–57

Salinger M J, Renwick J A and Mullan A B 2001 Interdecadal Pacific oscillation and south Pacific climate *Inter. J. Clim.* **21** 1705–21

Shi L, Ding R, Hu S, Li X and Li J 2023 Extratropical impacts on the 2020–2023 triple-dip La Niña event *Atmos. Res.* **294** 106937

Smith T M, Reynolds R W, Peterson T C and Lawrimore J 2008 Improvements to NOAA's historical merged land–ocean surface temperature analysis (1880–2006) *J. Clim.* **21** 2283–96

Stuecker M F 2018 Revisiting the Pacific meridional mode *Sci. Rep.* **8** 3216

Timmermann A *et al* 2018 El Niño–Southern Oscillation complexity *Nature* **559** 535–45

Vimont D J, Wallace J M and Battisti D S 2003 The seasonal footprinting mechanism in the Pacific: implications for ENSO *J. Clim.* **16** 2668–75

Wang B *et al* 2023 Understanding the recent increase in multiyear La Niñas *Nat. Clim. Change* **13** 1075–81

Wu Y K, Hong C C and Chen C T 2018 Distinct effects of the two strong El Niño events in 2015–2016 and 1997–1998 on the western North Pacific monsoon and tropical cyclone activity: role of subtropical eastern North Pacific warm SSTA *J. Geophys. Res. Oceans* **123** 3603–18

Wyrtki K 1985 Water displacements in the Pacific and the genesis of El Niño cycles *J. Geophys. Res. Oceans* **90** 7129–32

Xie S P 1999 A dynamic ocean—atmosphere model of the tropical Atlantic decadal variability *J. Clim.* **12** 64–70

Yeo S R and Kim S T 2021 Summer climate variability over Korea in association with diverse features of ENSO evolution *Clim. Dyn.* **56** 2823–38

You Y and Furtado J C 2017 The role of South Pacific atmospheric variability in the development of different types of ENSO *Geophys. Res. Lett.* **44** 7438–46

Zhang H, Clement A and Di Nezio P 2014 The South Pacific meridional mode: a mechanism for ENSO-like variability *J. Clim.* **27** 769–83

Zhang S, Fan H, Hu X and Lin S 2024 Unprecedented cross-equatorial southerly wind anomalies during the 2020–2023 triple-dip La Niña: impacts and mechanisms *Atmos. Res.* **304** 107412

Zhang Y, Amaya D J, Kosaka Y, Stuecker M F, Yang J-C, Lin X and Fan L 2022 Atmospheric forcing of the Pacific meridional mode: tropical Pacific-driven versus internal variability *Geophy. Res. Lett.* **49** e2022GL098148

Zheng Y, Chen S, Chen W, Wu R, Wang Z, Yu B, Hu P and Piao J 2024 The role of the Aleutian low in the relationship between spring Pacific meridional mode and following ENSO *J. Clim.* **37** 3249–68

Zhu T and Yu J Y 2022 A shifting tripolar pattern of Antarctic sea ice concentration anomalies during multi-year La Niña events *Geophys. Res. Lett.* **49** e2022GL101217